Performance evaluation of a combined ADCP- scientific echosounder system.

David Velasco, Briony Hutton, Dominique Lefèvre, Bruno Zakardjian, Carl Gojak, Karim Mahiouz, Celine Heyndrickx, Sven Nylund, Antoine Bezile

Performance evaluation of a combined ADCP-scientific echosounder system

David W. Velasco
Nortek Group
San Diego, USA
david.velasco@nortekgroup.com

Briony Hutton
Echoview Software Pty Ltd
Hobart, Australia

Dominique Lefevre
CNRS MIO
Marseille, France

Bruno Zakardjian
CNRS MIO
Marseille, France

Carl Gojak
Division Technique de L'INSU
La Seyne, France

Karim Mahiouz
Division Technique de L'INSU
La Seyne, France

Celine Heyndrickx
Division Technique de L'INSU
La Seyne, France

Sven Nylund
Nortek Group
Rud, Norway

Antoine Bezile
Nortek Group
Toulon, France

***Abstract*— Echosounders are widely used to quantify fish behavior, fish stocks, and zooplankton biomass. Acoustic Doppler Current Profilers have also been used to accurately measure currents in all of the world's major water bodies over the last 30 years. The present work evaluates the performance of a combined echosounder/ADCP system, the Nortek Signature100, for simultaneous biomass assessment and current profile data analysis.**

Due to its combined current profiling and scientific echosounding capabilities, the system is seeing increased usage in biomass flux applications, particularly in Antarctic krill research. However, capabilities of the system are still being studied and the present work aims to expand characterization of its performance. To that effect, a four month deployment was carried out by the French National Center for Scientific Research (CNRS) in the Mediterranean Sea with an up-looking Signature100 mounted atop the ALBATROSS mooring line. The line was at a total water depth of 2420 m and its top was approximately 370 m below the surface.

Data show significant variations in scattering conditions between daytime and nighttime due to diel vertical migration (DVM), often unrelated to horizontal velocity fluctuations, highlighting not only the multiple frequency band capabilities of the system (up to 7 bands), but also the strength of the combined echosounder and current profiling functions. Echoview, a commercial software package for hydroacoustic data processing, was used to further explore the spatial and temporal patterns of the organisms observed in the echosounder data. A semi-automated technique was implemented to efficiently and objectively clean (e.g. remove interference generated by passing ship traffic), classify (e.g. based on relative frequency response or morphology), and characterize the narrow bandwidth and pulse compressed echosounder data by generating outputs that can contribute to the management and monitoring of aquatic resources.

Keywords— scientific echosounding, ADCP, currents, biomass

I. INTRODUCTION

In terms of biomass, diel vertical migration (DVM) is potentially the largest animal migration on Earth [1]. Many planktonic species move through the epipelagic and mesopelagic zones, transiting up to and back down from the near-surface photic zone, following a regime closely tied to light cycles associated with day/night periods. This has been widely observed across all oceans and at various depths [2]-[3]. Interest in DVM has increased in recent years due to its role in the global ocean biological pump, as it contributes to the transfer of atmospheric CO_2 to the deep ocean not yet properly accounted for in climate models [4]-[5].

Since the 1980s, Doppler profilers have been used to observe DVM [6]-[10], with commercial Acoustic Doppler Current Profilers (ADCPs) used to complement traditional biological measurement techniques, such as conventional net sampling. This is due to the ability of ADCPs to collect current profiles as well as concurrent acoustic backscatter data, as these are heavily dependent on the quantity of particles (such as zooplankton) in the water column. Additionally, ADCPs are capable of operating autonomously for long periods of time (several months to years), and are not subject to the avoidance limitations common to net sampling.

The spatial resolution of traditional ADCPs has precluded their use for any detailed quantitative study of biomass distribution and abundance [11]-[13]. As such, they are often deployed together with scientific echosounders which are more capable of assessing biology within the water column. However, these two technologies (ADCPs and scientific echosounders) have historically been developed by separate companies, with different objectives, with the necessary integration left for the end user to handle. In an effort to reduce this complexity and increase the ease of use to the operator (and consequently, reduce cost), recent advances to combine ADCP and scientific echosounder technologies into a single instrument have opened the door to addressing some of these limitations [14]-[15]. Here we expand on this previous work [14], offering additional insights into the performance and capabilities of this new system.

II. SYSTEM DESCRIPTION

A detailed overview of the system has previously been presented in [14] and therefore here we provide a condensed

overview. The system belongs to the Signature Series family of ADCPs launched in 2013 by Norwegian scientific instrumentation company Nortek. It is powered by the AD2CP electronics platform (US Patent 7.911.880). The four slanted beams, responsible for profiling currents, operate at a center frequency of 100 kHz and can profile currents over a range of up to 400 m with 4 m spatial resolution and sampling rate up to 1 Hz.

The center vertical beam has a wider frequency band, from 70 to 120 kHz with a high dynamic range of 130 dB and supports different pulse types: 1) up to three discreet monochromatic pulses of 70 kHz (2.9% bandwidth), 90 kHz (2.2% bandwidth), and 120 kHz (1.7% bandwidth), and 2) a 90.9 kHz-centered chirp with 50% bandwidth with support for pulse compression. Up to three echograms can be recorded based on a user-defined mix between the different pulse types available (e.g. 70 kHz monochromatic, 120 kHz monochromatic, and 90.9 kHz-centered chirp).

The chirp pulse offers a selectable spatial resolution from 37.5 cm to 4.0 m. The pulse compression technique improves the signal-to-noise ratio (SNR) by compressing the longer transmit pulse which increases the transmitted energy output. The chirp can also be processed in up to five frequency bands of 10% bandwidth each, with center frequencies of 107.9, 99.4, 90.9, 82.3, and 73.8 kHz. This means the Signature100 provides up to seven different frequency bands that can be used in combination for applications including target classification and biomass assessment. Additionally, the Signature100 can store the demodulated in-phase (I) and quadrature-phase (Q) data from all echograms with configurable decimation such that user-defined processing techniques may be applied (e.g. combining the chirp with pulse compression to accurately establish distance to a calibration sphere; or processing the chip into more frequency bins). The system is shown on Fig. 1.

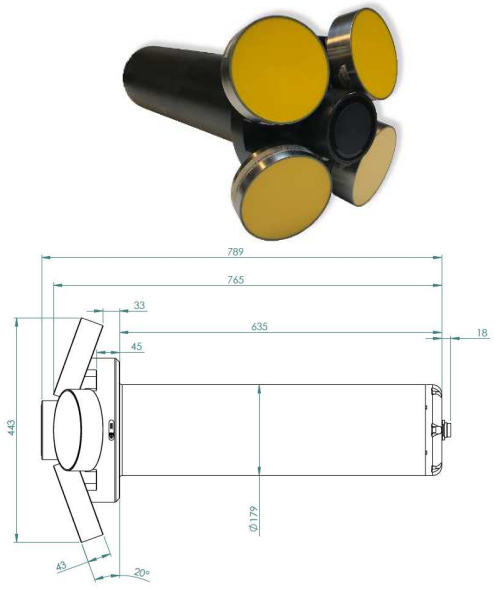

Fig. 1. Nortek's Signature100 ADCP. The four yellow transducers are responsible for measuring the currents. The center black transducer is a scientific echosounder. All dimensons in mm.

Because the term "narrowband" has different (and often ambiguous) implications when applied to ADCPs versus scientific echosounders, in this paper we avoid using the term "narrowband" in reference to either the 70, 90, or 120 kHz echosounder pulses generated by the Signature100. Instead, the term "monochromatic" is used throughout when referring to these pulses, referencing their transmit characteristic.

III. Deployment Setup

In order to further characterize the Signature100's capabilities, a four-month deployment was done by the French National Center for Scientific Research (CNRS) from 24/Aug/2019 and 03/Jan/2020 in the western Ligurian Sea (northwest Mediterranean Sea). The instrument was installed atop the Autonomous Line with Broad Acoustic Transmission for Research in Oceanography and Sea Sciences (ALBATROSS) mooring. The ALBATROSS mooring is part of the European Multidisciplinary Seafloor and water column Observatory (EMSO), specifically the EMSO-Western Ligurian Sea regional facility (https://www.emso-fr.org/EMSO-Western-Ligurian-Sea). The mooring is located at 42° 48.3730' N and 6° 01.6098' E at a seafloor depth of 2420 m (Fig. 2), and the Signature100 was in a subsurface buoy atop the mooring, up-looking, positioned approximately 370 m below the sea surface.

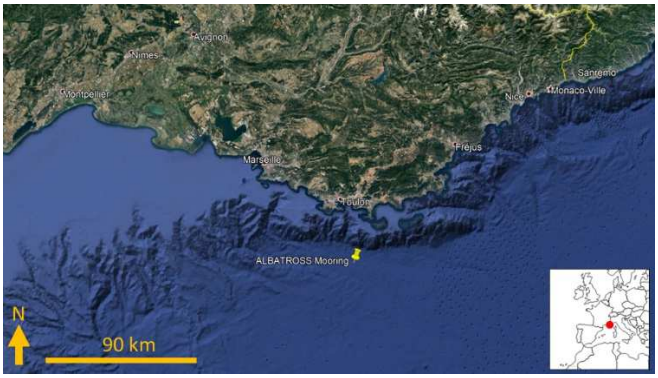

Fig. 2. Location of ALBATROSS mooring with Signature100 just south of Toulon, France.

The Signature100 was configured with a concurrent current profiling and scientific echosounder sampling regime. The ADCP portion of the instrument was configured to transmit 40 pings with 6.25% bandwidth (Long Range mode) at 0.16 Hz evenly spread over an averaging interval of 240 s. This sequence was repeated every 30 minutes. Depth cell size was 5 m and a total of 90 cells were collected, with a blanking distance of 2 m. At this depth cell size, if all 40 pings are considered valid within an ensemble (see discussion in section IV.A), they provide a theoretical horizontal and vertical velocity precision of 2.62 cm/s and 0.68 cm/s, respectively. All single ping data are recorded by default for the Signature100 onboard a microSD card.

The scientific echosounder portion of the instrument was configured to transmit a 90.9 kHz-centered wideband (50% bandwidth) chirp of 6 ms duration, with pulse compression applied, and storage of in-phase (I) and quadrature-phase (Q) components of the return signal at 45.45 kHz (50% of the center frequency). The pulse was processed in the five

supported frequency bands. In addition to the chirp, a 70 kHz monochromatic pulse of 1 ms duration was also transmitted one second after the chirp. Both pulses were transmitted continuously throughout the four-month deployment at 12 s intervals, and each return was recorded in 597 depth cells of 0.75 m size. A third monochromatic pulse was also configured, but due to a user configuration mistake it was also set to 70 kHz, rather than a complimentary 90 or 120 kHz frequency, thus unfortunately returning minimal additional information (although the 1 s separation between the two 70 kHz pulses did offer some glimpses at the movement of scatterers; not presented). For this deployment, the echosounder was not calibrated either prior or post deployment and therefore data have not received any calibration offset (see Section V. A. for details).

Data collection for the Signature100 was initiated on 20/Aug/2019 and the mooring deployed on the morning of 24/Aug/2019 (all times in this paper are UTC). Retrieval was on the afternoon of 03/Jan/2020. During these 136 days the instrument generated a total of 62 GB of data, with 61.5 GB (99.2%) being the echosounder data and 0.5 GB (0.8%) being the ADCP data. Power was supplied by Lithium battery packs providing a combined capacity of 1800 Wh. Power consumption for this configuration totaled 1761.9 Wh, with 1409.5 Wh (80%) used to power the echosounder and 352.4 Wh (20%) to power the ADCP.

IV. ADCP Data

A. Data Processing

Single-ping data from the Signature100's slanted beams (responsible for the velocity measurement) were post-processed with Nortek's OceanContour software. The first step was to transform the data into appropriate Earth-reference coordinates and applying a +2° magnetic declination. The second step was to mask any depth cell along all four beams with the following thresholds: a) signal correlation below 50%, and b) range within 7% of the surface to avoid sidelobe interference. Signal correlation is a statistical measure of the similarity between the first and second pulses in the pulse pair used to measure velocity, and it is output as a percentage. Data above 50% is considered of good quality. The third step was to ensemble average all individual pings over the 240 s averaging interval. As part of this averaging process, a Percent Good value is generated representing a collection of all individual pings within an ensemble that have passed the earlier thresholds. For the configuration used in this particular deployment, especially as it concerns the depth cell size used, the horizontal velocity precision σ_H is given by:

$$\sigma_H = \frac{16.594}{\sqrt{N}} \qquad (1)$$

where N is the number of valid pings averaged in a given ensemble. For example, if all 40 pings in the ensemble are valid, then the maximum precision of 2.62 cm/s will be achieved. A review of the entire deployment yielded 91% of the horizontal velocities within the first 3 depth cells (where velocities were slowest) were above 4.70 cm/s. A 12-ping average over the ensemble provides a horizontal velocity precision of 4.79 cm/s. Therefore, only data with a Percent Good value above 30% (i.e. 12/40) were taken as part of the third processing step. Of all 6348 ensembles recorded, 4599 had at least 35 valid pings, meaning that >72% of the data have a precision of 2.8 cm/s or better.

B. Data Review

An initial overview of the current data is presented in Fig. 3 where 24-hr averages of current speed and direction are shown along with signal correlation and amplitude for beam 1 only (beam 1 was chosen for simplicity; all four beams reported comparable values).

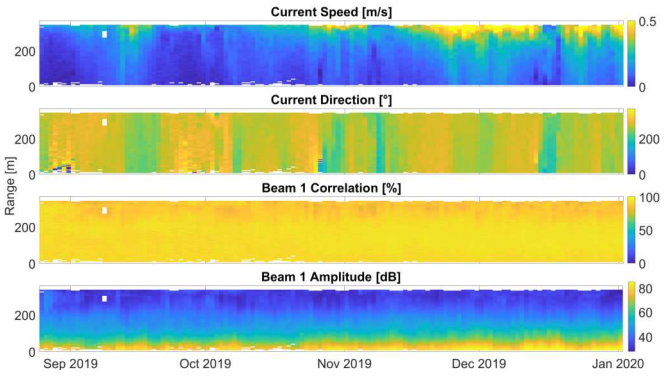

Fig. 3. Daily averages of current speed, current direction, Doppler signal correlation and signal amplitude.

From this overview we can observe how velocities are higher towards the surface, as expected, reaching speeds above 50 cm/s at times. Flow direction is mostly uniform with depth and often to the west, with occasional episodes to the southwest. Signal correlation and amplitude data show strong values as expected due to earlier masking during initial post-processing. However, noticeable periods of invalid data found in the daily averages towards the first several cells of the profiling range highlighted the need for a more comprehensive analysis of the higher resolution 240 s ensemble average data.

A review of the ensemble averaged current data presents two noticeable aspects: reduction in current profiling range over any given 24-hour period with an additional seasonal component, and decorrelation within the first several depth cells. To understand the first aspect (range reduction), we first must understand that ADCPs depend on particles in the water column to operate. These particles must have an acoustic impedance sufficiently different than the surrounding water to be detectable by any acoustic system. For example, suspended sediments, fish, and zooplankton are typically strong acoustic scatterers, while phytoplankton are often acoustically transparent to an ADCP. As such, water that is lacking in "valid" scatterers pose a challenge to such systems. It is important to note, however, that lack of scatterers does not inherently degrade an ADCP's velocity data quality but rather only impacts its maximum usable profiling range [16]. While a complete absence of acoustic scatterers in natural waters is uncommon, it has long been observed that some water bodies contain limited (and variable) quantities of scatterers, thus impacting an ADCP's range [17], [18]. The Mediterranean Sea is one such location. While zooplankton are indeed good scatterers and are abundantly present in the Mediterranean, especially copepods [19], [20], the lack of significant riverine

input (adding suspended sediment) means that zooplankton are likely the primary acoustic scatterers in the Mediterranean Sea. Therefore, the temporal and spatial distribution of biological scatterers is a significant influencer in an ADCP's practical maximum profiling range in this location (Fig. 4, 5).

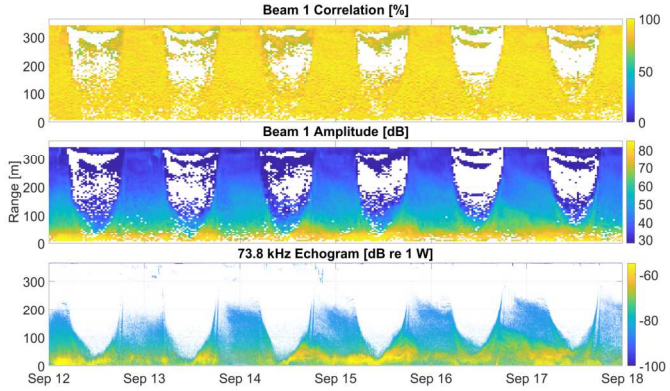

Fig. 4. Signal correlation, amplitude (both from slanted beam 1), and echogram from the 73.8 kHz-centered frequency band of the chirp for a 6-day period in September 2019. Correlation and amplitude are from ensemble averaged data recorder every 30 minutes, while echogram unaveraged (recorded every 12 s). Note dB scales are not interchangeable between echogram and signal amplitude.

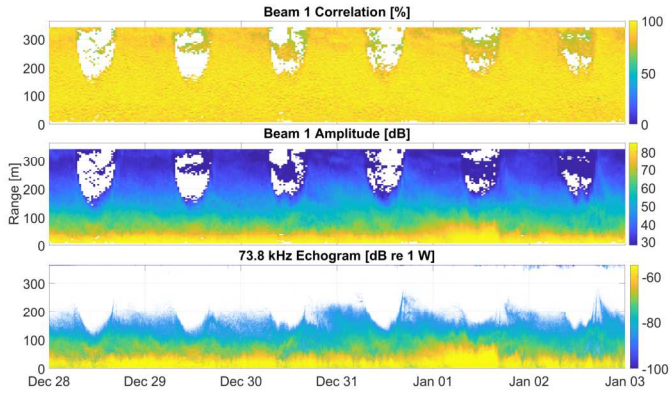

Fig. 5. Same as Fig. 4, except for late December 2019.

In Fig. 4 and Fig. 5, two 6-day long periods during the deployment are shown. Fig. 4 is from mid-September 2019 (autumn in northern hemisphere), and Fig. 5 is from late December 2019 and into early January 2020 (winter). Signal correlation and signal amplitude for one of the slanted beams (beam 1) are plotted over time in each figure. Current data not meeting the earlier stated thresholds were excluded and appear as white areas in each plot. These figures show how valid data extends all the way to near the surface (full range) during night hours, but is noticeably reduced during daylight hours. The bottom plot of Fig. 4 and Fig. 5 shows the processed echogram from the 73.8 kHz band of the chirp, transmitted from the center beam (see section V for details on the processing applied). The echogram suggests that the loss of velocity profiling range is related to DVM of zooplankton and other animals as a function of light (day/night) cycles. As the animals migrate upward in the water column, its acoustic scattering potential increases allowing for the profiler to achieve full range. Around sunrise the pattern reverses and profiling range is therefore reduced. The pattern also varies with season, as there is more biomass in the upper water column during shorter winter days (Fig. 5) than during autumn months (Fig. 4), therefore range reduction of current profiling is less in winter. The apparent shorter range of the echogram at night when compared to the ADCP signal amplitude is an artifact of the processing used on the echosounder data, in particular the noise threshold used (see Section V). However, echosounder pulses reached the surface both during the day and night, as evidenced by the near-surface reflectors seen in both Fig. 4 and Fig. 5.

To further illustrate the daily range fluctuations, we show the maximum current profiling range as a function of time of day on Fig. 6. The full range is effectively always achieved during nighttime hours, while full range is only partially achieved during the day, at times being only up to approximately 100 m above the instrument (a 75% reduction in the maximum nominal range of 400 m).

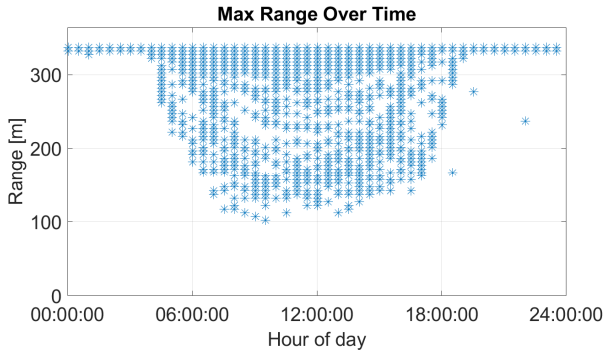

Fig. 6. Maximum current profiling range over time as a function of time of day. Maximum nominal range for the Signature100 is 400 m in optimal scattering conditions. Instrument was deployed approximately 370 m below the sea surface.

The second aspect observed in the current profiling data, namely decorrelation within the first several depth cells above the instrument, is presumed to be due to lack of scatterers and presence of sizeable reflectors near the instrument. Fig. 7 shows the processed echogram from the 73.8 kHz-centered band for a one-hour interval during the morning of 14/Sept/2019, for a range of 100 m above the instrument. Large reflectors are readily seen, presumed to be both small schools of fish or zooplankton, and individual fish. Regions between reflectors show significantly lower signal strength, and concentrated strong reflectors pose a challenge to the statistical calculations of Doppler processing techniques, especially if they are swimbladdered fish [21], [22]. While fish rejection algorithms can address some of these cases, they are not capable of completely eliminating this interference, resulting in some data loss [23],[24]. Above approximately 50 m range most of the signal is below the minimum threshold (see section V), further indicating water with very few scatterers, contributing to the reduced velocity profiling range.

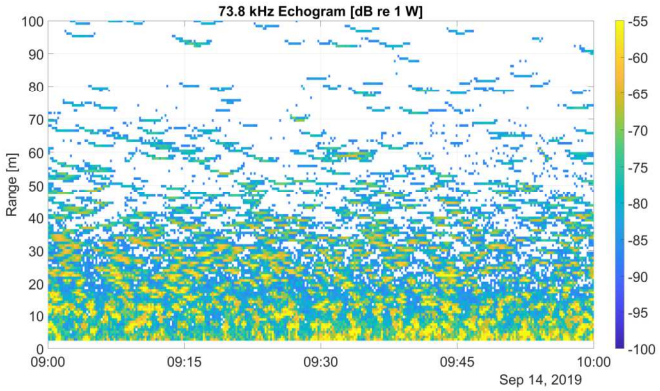

Fig. 7. Processed 73.8 kHz-centered frequency band for one hour during the morning of 14/Sept/2019, over a 100 m range above the Signature100. Large reflectors are readily observed, swimming in water with lower signal strength.

C. *Vertical Velocity*

While some advanced methods inferring DVM velocities have been proposed [9], in this work we take a more direct approach by using the vertical velocities directly measured by the Signature100, focusing on times prior to sunrise and sunset, as determined from the nearest meteorological station (Toulon, France). An initial analysis ruled out any migratory motion after sunrise and after sunset. Vertical velocities were taken for every ensemble average interval, and not averaged over weekly intervals. Organisms in this part of the Mediterranean Sea appear to start their upward migration up to six hours before sunset (Fig. 8), increasing in speed as sunset approaches, reaching up to 5 cm/s (Fig. 9). By the time the sun has risen, they have completed their journey. They then descend at a slightly slower rate of approximately 4 cm/s and appear to begin their journey within four hours prior to sunrise. Opposite of their ascent sequence, they appear to move faster at the start of their descent then at the end. Additionally, speeds are noticeably higher during autumn (September) than later in winter (December).

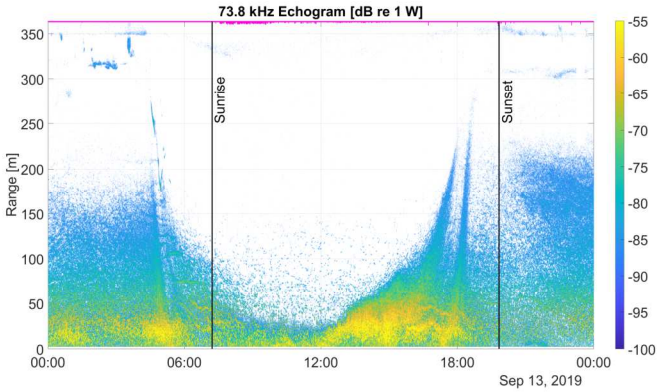

Fig. 8. Processed 73.8 kHz-centered frequency band showing a typical descend/ascend DVM sequence. Magenta area is unwanted backscatter from entrained air near surface. Local sunrise and sunset times are indicated by vertical lines.

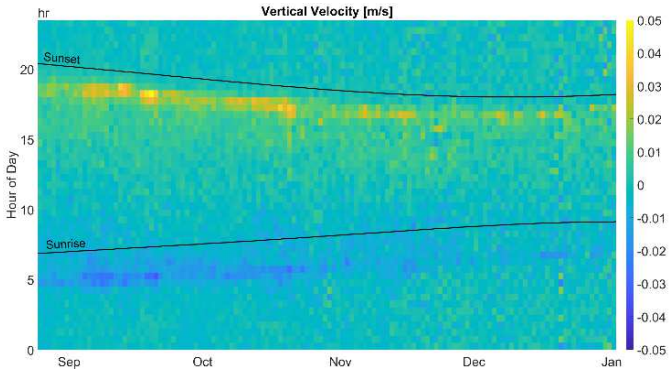

Fig. 9. Vertical velocity measured by the Signature100 as a function of time of day and month. Times for sunrise and sunset at the nearest meteorological station (Toulon, France) are shown. Increase in upward and downward speed is readily seen to follow these lines.

V. Echosounder Data

A. *Data Processing*

Echosounder data recorded by the Signature100 was processed using Echoview® 12.0.304 (Echoview Software Pty Ltd, Hobart, Australia). Echoview 12 enables post processing of data from Signature100 files that represent monochromatic measurements from a narrow frequency band, as well as the processed, pulse compressed measurements from five wider-frequency bands (chirps). Heading, pitch, and roll measurements for the transducer platform are available, but were not used in this analysis. Tilt during the deployment was negligible: mean pitch was -0.4° (standard deviation 0.05°) and mean roll was -0.16° (standard deviation 0.05°). Echoview's platform configuration settings were used to identify the transducer orientation as an upwards-facing platform, and a nominal 370 m vertical offset was applied to position the transducer correctly in the water column, allowing the conversion of sample range (distance from transducer face) to depth (distance from the water surface). Data from 25/Aug/2019 07:02:27 until 03/Jan/2020 15:28:51 were used in the echosounder analysis and comprised 945,734 pings of data recorded to 450 m range.

1) *Monochromatic Data*

For Signature100 monochromatic measurements, Echoview calculates and provides variables that represent power (dB re 1 W), target strength, TS (dB re 1 m^2), and volume backscattering strength, S_v (dB re 1 m^2/m^3). TS and S_v are calculated from power by applying standard sonar equations as described in [16]. TS data can be used to count and analyze individual targets when conditions allow (i.e. sufficiently low numbers of fish in the acoustic sampling volume), which was observed during this deployment but not presented in this paper. The monochromatic 70 kHz S_v data were analyzed, and as the echosounder was not calibrated, a nominal -40 dB offset was applied to the sample values to shift backscatter to a more typical amplitude range. All references to S_v in this analysis should therefore be regarded as an approximate rather than absolute measure of volume backscatter. Absolute measurements can be achieved using calibrated data, as described in [15].

The sample data also contained strong signals from non-scattering sources, such as acoustic and electrical interference from passing vessels. Echoview's built-in algorithms were used to classify and address spikes of impulse noise. Entire pings that were automatically identified as a factor of 2 stronger than surrounding pings were removed. Within-ping spikes of strong backscatter were classified as noise if they were 8 dB higher than the mean backscatter in a window of samples 7 pings wide by 2 m tall, and these spikes were replaced with the mean of surrounding pings using the algorithms described in [25].

Background noise is an artifact of increasing sound attenuation with increasing distance from the transducer, resulting in a reduced SNR and the presence of a background noise gradient in sample data that can vary due to weather conditions and other influences [26]. Background noise was estimated and subtracted based on a cell size of 50 pings wide by 1 meter tall and an SNR threshold of 12 dB. The data were smoothed to reduce the effect of stochastic variation by applying a top-hat convolution calculated from the 8 samples immediately surrounding each sample.

Standard water column echosounder data processing typically requires the delineation of exclusion lines to ensure that transducer ringing and backscatter from the water surface, seafloor, or other such boundaries do not contribute to biological estimates, as reflectivity of these boundaries is usually significantly stronger than biological sources. The lower boundary of the water surface was automatically detected to remove water surface backscatter from further analysis. Starting from the transducer face, samples in each ping were searched to find the depth of the first sample that was greater than 300 m away (i.e. above the instrument) and stronger than -20 dB. As near-surface noise (likely due to entrained air bubbles from breaking waves) sometimes extended further into the water column at a lower strength, a second search was then performed to find the extended depth at which backscatter dropped to -90 dB, then an additional 1 m was added as an offset. It should be noted that this process may have eliminated some backscatter from biological sources if they were very close to the surface yet indistinguishable from entrained bubbles. A line was created that joined the resulting depths across all pings, and this line was used to exclude backscatter from surface and entrained air from further analysis (magenta region in applicable figures). For the lower boundary of the sampled water column, the samples closest to the transducer face contained no noise or ringing due to the user-defined blanking distance set when data was recorded, and therefore no close-range exclusion line was required. Finally, the echogram for the full deployment was manually reviewed and edited for any remaining instances where the automatic noise removal and surface exclusion algorithms underperformed, and an analysis threshold of -90 dB was applied. Fig. 10 shows echograms comparing the original S_v measurements to the same selection of data after noise and unwanted backscatter were removed.

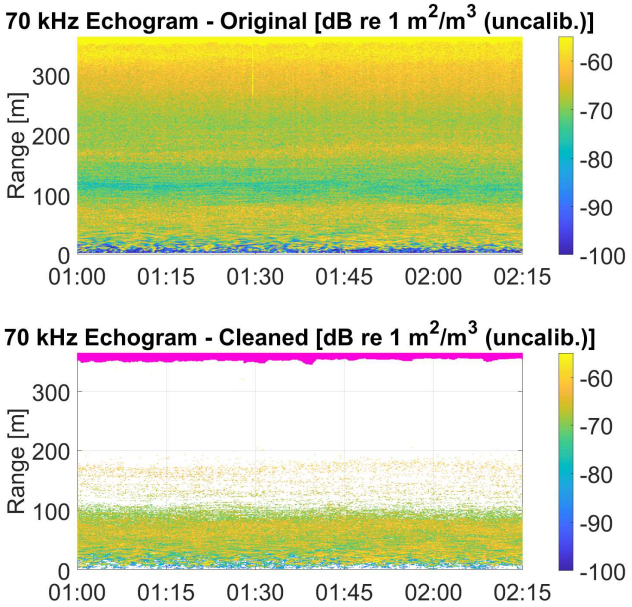

Fig. 10. Echogram from 70 kHz monochromatic pulse showing original data (top panel) and then processed (bottom panel) to remove background noise, impulse noise, unwanted backscatter from entrained air near surface (shown in magenta) and the water surface itself, and below-threshold values. All data from 13/Nov/2019 and all times in UTC.

The cleaned S_v data for the full deployment were averaged to 100 bins in the depth dimension (each 4.47 m thick) by 30 minutes in the temporal dimension and exported to a comma-separated values (CSV) file. The 6-day long winter and autumn periods were exported to CSV files at original (not averaged) resolution. The full deployment and depth extent of the water column was analyzed in 30-minute intervals using the approach and equations detailed in [27], which describes useful metrics to characterize vertical distribution patterns in temporal data. Mean S_v, aggregation index, center of mass, equivalent area, inertia, and proportion occupied were examined for the full length of the deployment. Additionally, changing temporal patterns in these metrics were examined using the WaveletComp package [28] in R, a wavelet-based analysis tool that enables visualization of periodicities in time series data.

2) Processed Pulse Compressed Data

Echoview derives one variable for each of the processed, pulse compressed and bandpass-filtered bins of data recorded to file, and the nominal center frequency for each band is identified. The sonar equation is not applied to this data type in Echoview, and data values were in a typical amplitude range so no dB offsets were required. Data from all 5 bands were processed in an identical manner.

As with the monochromatic data, Echoview's built-in algorithms were first used to identify and remove entire pings that contained erroneously high measurements, and to replace spikes within pings with the mean of surrounding samples. As the S_v equation is not applied to this data type, a constant -88 dB threshold was applied to samples at all ranges to mitigate the background noise component in the data.

The near-surface exclusion line calculated for the monochromatic data was also used to exclude the water surface and entrained air from the processed pulse compressed data analysis. A fixed-depth line was used to exclude the saturated backscatter in the first 3 samples. The cleaned sample data for the week-long winter and autumn periods were exported to CSV files at original data resolution.

B. Data Review

The 70 kHz monochromatic measurements provided a wide variety of meaningful insights into biological activity in the deployment data. Distinct DVM processes were visible at the start of the deployment in August, with the bulk of the biomass ascending between 14:00 and 16:00 and descending between 04:00 and 06:00 (all times in UTC); reference sunrise/sunset times in Fig. 9. During the daylight hours, large individual targets were visible between 65 and 125 m above the instrument, and at all hours of the day between 0 and 65 m. During the night, dense aggregations of very strongly-scattering targets were often observed at 283 to 365 m above the instrument (i.e., from the water surface to 82 m below the surface). This pattern continued until late October when the intensity of the migrating backscatter reduced, and a consistent layer appeared that extended from the instrument to 115 m above it. Far fewer individual targets were distinguishable on the boundaries of the layer, and strongly-scattering aggregations at far range (i.e., in the surface waters) were rare. By the end of the deployment in winter, a dense layer of biology was present from the instrument to 165 m above it, with sub-layers visible within, and DVM was heavily reduced in intensity. Individual targets could only be resolved close to the transducer face. Strong targets or aggregations were not observed in the upper 200 m of the water column after 19/Nov/2019, other than one ascending, very large individual scatterer (such as a marine mammal) or aggregation on the afternoon of 28/Nov/2019 as seen on Fig. 11.

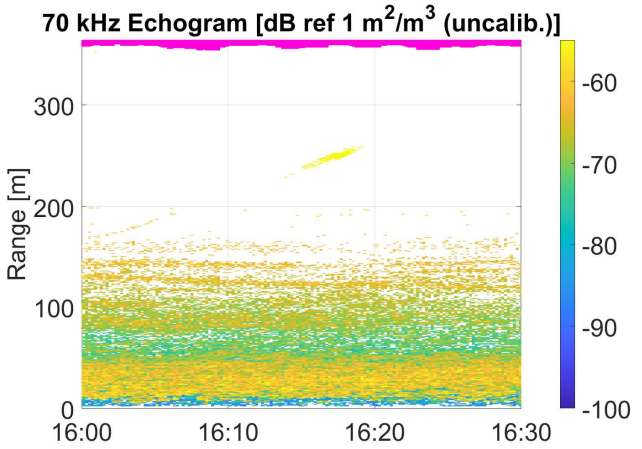

Fig. 11. Echogram from 70 kHz monochromatic pulse showing a strongly scattering target ascending above the instrument. Target is presumed to be either a large, single marine mammal or an aggregation of animals. Magenta area is unwanted backscatter from entrained air near surface. All data from 28/Nov/2019 and all times in UTC.

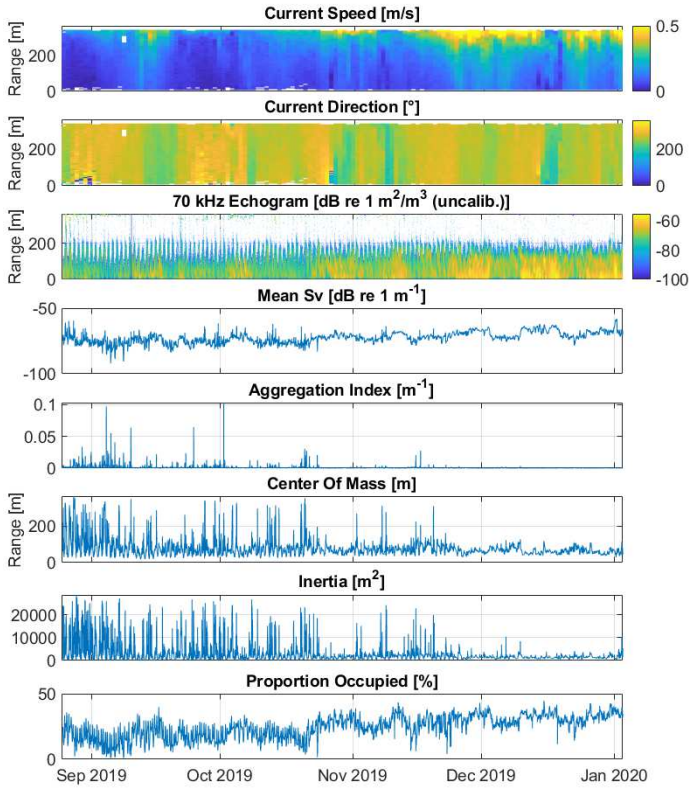

Fig. 12. Current speed, current direction and the monochromatic 70 kHz Echogram, plus key "Echometrics" from Echoview software. Mean Sv is a proxy for biomass, Aggregation Index is a measure of patchiness, Center of Mass shows the average depth of backscatter weighted by backscattering strength, Inertia is the spread of biomass from the center of mass, and Proportion Occupied is the percentage of the water column that contains backscatter.

The metrics used to characterize the vertical distribution patterns throughout the deployment highlighted several temporal patterns (Fig. 12). Mean S_v, a proxy for biomass, was slightly lower but more variable in the first half of the deployment, and higher but less variable in the second half. Center of mass (the average range of the backscatter weighted by backscattering strength), covered the full extent of the sampled water column in a cyclic pattern from the start of the deployment until 19/Nov/2019 with decreasing frequency, and was less than 158 m (i.e. deeper than 207 m from the sea surface) for the remainder of the deployment. Center of mass was less than 115 m from the system during the 6-day long winter period. Inertia (spread of biomass from the center of mass) followed a similar pattern. Proportion occupied (the percentage of the water column that contains backscatter) was an average of 18% for the deployment period up to and including 23/Oct/2019 and increased to 30% after this date. During the 6-day long autumn period, a clear daily pattern could be seen that cycled between 10% and 40% coverage, whereas the winter period varied between 28% and 42% in a less regular cycle. Aggregation index (0 identifies evenly distributed backscatter and 1 identifies small and dense schools) was more variable prior to 23/Oct/2019, and tended to 0 after this date. Similar trends were observed in the wavelet analyses (Fig. 13). They also enabled other temporal patterns to be elucidated, for example, proportion occupied

contained an orange-red band at the top of the plot (Fig. 13f) that indicated a lunar and/or tidal periodicity in water column occupation, and the strong red band in the lower third of the plot at half-day intervals for the first half of the deployment highlighted a very strong diurnal periodicity, which reduced in intensity from late October until the end of the deployment. Center of mass showed a strong 12- and 24-hour periodicity up until late October, which then reduced and/or disappeared entirely.

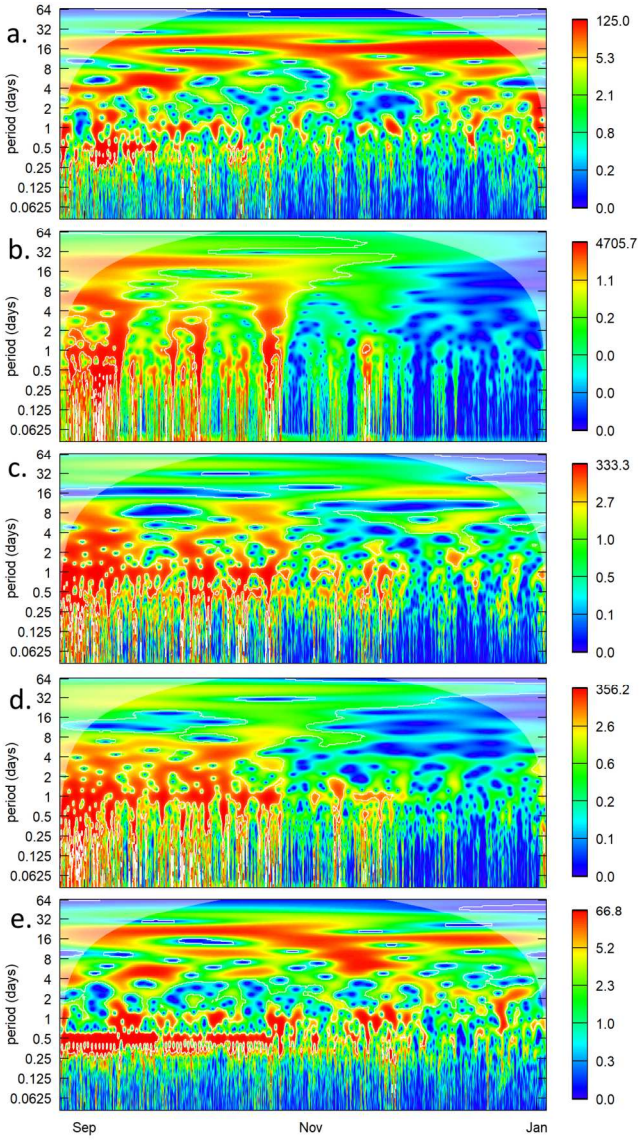

Fig. 13. Wavelet transform of the key metrics in 30 minute intervals for the deployment. Plot a is Mean Sv, b is Aggregation Index, c is Center of Mass, d is Inertia, and e is Proportion Occupied (see Fig. 12 caption for descriptions). Regions of significance (significance level = 0.1) that suggest periodicity, and the "cone of influence" (white transparent overlay; data points that are subject to the risk of edge effects) are highlighted in these plots. Higher wavelet power values indicate stronger periodicities in the dataset at the given time.

Very similar temporal patterns were observed in the processed pulse compressed data. Individual targets were more clearly vertically resolved, suggesting better potential for echo-counting techniques. The backscatter for the DVM component of the data in the 73.8 kHz nominal frequency echograms was typically 2.5 to 4.6 dB stronger than the 107.9 kHz nominal frequency echograms throughout the deployment (as can be seen on Fig. 14), indicating that targets throughout the time series have similar scattering properties, which may suggest that the community is comprised of the same or similar organisms across seasons.

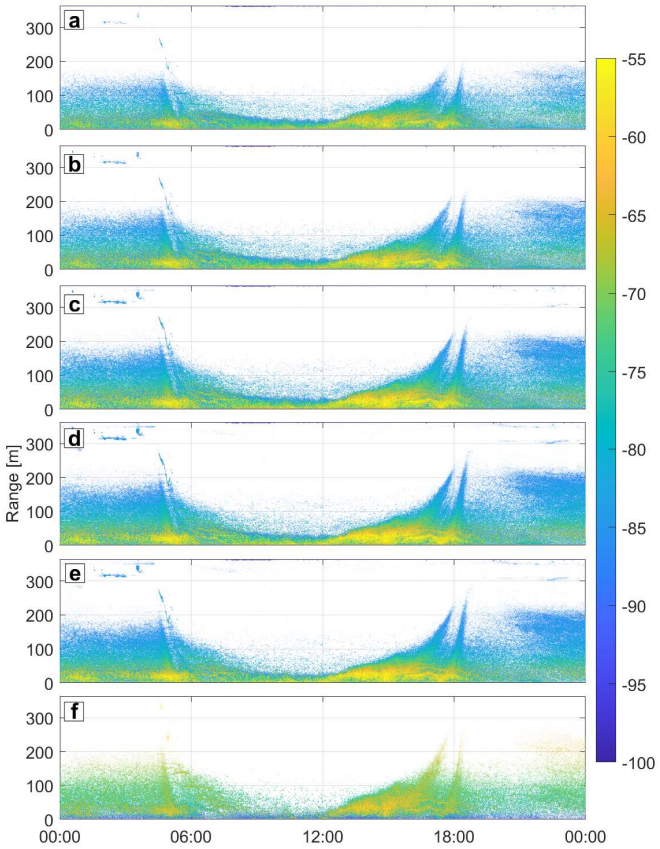

Fig. 14. Cleaned echograms for all five processed pulse compressed frequency bands, with a-e being 107.9 kHz, 99.4 kHz, 90.9 kHz, 82.3 kHz, and 73.8 kHz nominal frequencies, respectively, in units of dB re 1 W. Plot f is from the monochromatic 70 kHz pulse in units of dB re 1 m^2/m^3 (uncalibrated), with a -40 dB offset applied. All data from 13/Sept/2019 and all times in UTC. Colorbar range applies to all plots.

VI. Conclusions

This work presented a combined echosounder/ADCP system capable of profiling currents and imaging biology within the water column. Data from a four-month deployment in the Ligurian Sea (northwest Mediterranean Sea) of a Nortek Signature100 system was examined. The system was mounted atop a mooring and positioned up-looking approximately 370 m below the surface. The deployment lasted from late August 2019 to early January 2020. Review of the data was separated into two sections, covering first the ADCP portion of the instrument and then the scientific echosounder portion.

Current data show flows were higher towards the surface, reaching speeds above 50 cm/s and generally flowing to the west, with minor variations in depth. Two clear aspects were observed: reduction in current profiling range over 24-hour periods, and signal decorrelation within the first several depth

cells. Variability in current profiling range was closely related to diel vertical migration (DVM) of marine species and associated with day/night periods, confirming how biology is a strong influencer of ADCP range in the Mediterranean (and likely other "clear water" bodies). Full profiling range was achieved during nighttime hours, while full range was only partially achieved during daylight hours. Range reduction of up to 75% was observed during some daylight hours at times. While the study did not cover a full annual cycle, a seasonal signal (from autumn into winter) was observed, with winter months providing a higher percentage of current profiles achieving full range than autumn months. Although species identification was not performed, copepods make up the largest zooplankton community in the Mediterranean and a relationship between zooplankton community composition and seasonal variability in current profiling range may exist.

The echosounder portion of the instrument was configured to transmit and record a 70 kHz monochromatic pulse of 1 ms duration, as well as a 90.9 kHz-centered wideband (50% bandwidth) chirp of 6 ms duration. Pulse compression was applied to this chirp, and storage of raw I/Q data. While the echosounder data were not calibrated against a reference target (i.e. a calibration sphere), the data nonetheless contain a wealth of information. Both monochromatic and pulse compressed echosounder data were post-processed with Echoview software following standard procedures. Data were cleaned to remove background noise, impulse noise, unwanted backscatter near the sea surface, the sea surface itself, and other below-threshold noise. Metrics were computed to characterize the vertical distribution patterns and further describe both the daily as well as the seasonal variation in biomass during the deployment. A wavelet analysis was also performed, highlighting other periodicity related to lunar and/or diurnal fluctuations.

Overall, we conclude the Signature100 offers valid current profiling data coupled with scientific echosounder data, providing a wide variety of meaningful insights into the physical oceanographic characteristics and biological activity at the deployment site.

VII. Acknowledgements

The authors would like to thank Haley Viehman for assistance with the Wavelet analysis, as well as all the field crew responsible for the successful deployment and recovering of the ALBATROSS mooring containing the Signature100. The EMSO Western Ligurian project is supported by the French Oceanographic Fleet (EMSO-ANTARES project, DOI 10.17600/18001080).

VIII. References

[1] G. C. Hays, "A review of the adaptive significance and ecosystem consequences of zooplankton diel vertical migrations," 2003, Hydrobiologia, Vol. 503, pp. 163–170, doi: 10.1023/B:HYDR.0000008476.23617.b0.

[2] D. Bianchi, K. A. S. Mislan, "Global patterns of diel vertical migration times and velocities from acoustic data," Limnol. Oceanogr., 2016, 61:353-364, doi: 10.1002/lno.10219.

[3] J. Ochoa, H. Maske, J. Sheinbaum, J. Candela, "Diel and lunar cycles of vertical migration extending to below 1000 m in the ocean and the vertical connectivity of depth-tiered populations," Limnol. Oceanogr., 2013, 58(4):1207-1214, doi: :10.4319/lo.2013.58.4.1207.

[4] J. T. Turner, "Zooplankton fecal pellets, marine snow, phytodetritus and the ocean's biological pump", 2015, Progress in Oceanography, Vol 130, pp. 205-248, doi: 10.1016/j.pocean.2014.08.005.

[5] D. Bianchi, E. Galbraith, D. Carozza, K. A. S. Mislan, C. A. Stock, "Intensification of open-ocean oxygen depletion by vertically migrating animals", 2013, Nature Geoscience Vol. 6, pp. 545–548, doi: 10.1038/ngeo1837.

[6] A. J. Plueddemann, R. Pinkel, "Characterization of the patterns of diel migration using a Doppler sonar", Deep Sea Research Part A. Oceanographic Research Papers, Vol. 36, Issue 4, 1989, pp. 509-530, doi: 10.1016/0198-0149(89)90003-4.

[7] C. N. Flagg, S. L. Smith, "On the use of the acoustic Doppler current profiler to measure zooplankton abundance", Deep Sea Research Part A Oceanographic Research Papers, Vol. 36, Issue 3, 1989, pp. 455-474, doi: 10.1016/0198-0149(89)90047-2.

[8] C. D. Wilson, E. Firing, "Sunrise swimmers bias acoustic Doppler current profiles," 1992, Deep-Sea Research, Vol. 39, No. 5, pp. 885-892, doi: 10.1016/0198-0149(92)90127-F

[9] J. Luo, P. B. Ortner, D. Forcucci, S. R. Cummings, "Diel vertical migration of zooplankton and mesopelagic fish in the Arabian Sea", Deep Sea Research Part II: Topical Studies in Oceanography, Vol. 47, Issues 7–8, 2000, pp. 1451-1473, doi: 10.1016/S0967-0645(99)00150-2.

[10] B. Cisewski, V. H. Strass, M. Rhein, S. Krägefsky, "Seasonal variation of diel vertical migration of zooplankton from ADCP backscatter time series data in the Lazarev Sea, Antarctica", Deep Sea Research Part I: Oceanographic Research Papers, Vol. 57, Issue 1, 2010, pp. 78-94, doi: 10.1016/j.dsr.2009.10.005.

[11] L. Zedel, T. Knutsen, R. Patro, "Acoustic Doppler current profiler observations of herring movement", ICES Journal of Marine Science, Vol. 60, Issue 4, 2003, pp. 846–859, doi: 10.1016/S1054-3139(03)00067-5.

[12] C. Smyth, A. E. Hay, P. S. Hill, D. Schillinger, "Acoustic observations of vertical and horizontal swimming velocities of a diel migrator", Journal of Marine Research, Vol. 64, No. 5, 2006, pp. 723-743(21), doi: 10.1357/002224006779367258.

[13] B. Cisewski, H. Hátún, I. Kristiansen, B. Hansen, K. M. H. Larsen, S. K. Eliasen, J. A. Jacobsen, "Vertical Migration of Pelagic and Mesopelagic Scatterers From ADCP Backscatter Data in the Southern Norwegian Sea", Frontiers in Marine Science, Vol. 7, 2021, doi: 10.3389/fmars.2020.542386.

[14] D. W. Velasco, S. Nylund and T. Pettersen, "Combined Current Profiling and Biological Echosounding Results from a Single ADCP", 2018 OCEANS - MTS/IEEE Kobe Techno-Oceans (OTO), 2018, pp. 1-5, doi: 10.1109/OCEANSKOBE.2018.8559356.

[15] G. Cutter, S. Nylund, C. Reiss, D. Velasco, "Calibration, operation, and analysis of data from the Nortek Signature100 ADCP to estimate biomass and transport of Antarctic krill", AGU Ocean Sciences Meeting, San Diego, CA, USA, February 20 2020, Poster OB44D-0703.

[16] Nortek, "Principles of Operation – Signature", 2021, version 2021.1, https://support.nortekgroup.com/hc/en-us/articles/360029835831-Principles-of-Operation-Signature, accessed 08/July/2021.

[17] J. Fischer, M. Visbeck, "Deep Velocity Profiling with Self-contained ADCPs", 1993, Journal of Atmospheric and Oceanic Technology, Vol. 10, Issue 5, pp. 764-773, doi: 10.1175/1520-0426(1993)010<0764:DVPWSC>2.0.CO;2.

[18] D. E. DiMassa, B. A. Magnell and J. M. Lund, "Effects of temporal and vertical variability of echo amplitude on ADCP selection and performance," MTS/IEEE Oceans 2001. An Ocean Odyssey. Conference Proceedings (IEEE Cat. No.01CH37295), 2001, pp. 922-929 vol.2, doi: 10.1109/OCEANS.2001.968240.

[19] A. Nowaczyk, F. Carlotti, D. Thibault-Botha, M. Pagano, "Distribution of epipelagic metazooplankton across the Mediterranean Sea during the summer BOUM cruise," 2011, Biogeosciences, Vol. 8, pp. 2159–2177, doi: 10.5194/bg-8-2159-2011

[20] I. Siokou-Frangou, U. Christaki, M. G. Mazzocchi, M. Montresor, M. Ribera d'Alcalá, D. Vaqué, A. Zingone, "Plankton in the open

Mediterranean Sea: a review," 2010, Biogeosciences, Vol. 7, pp. 1543–1586, doi: 10.5194/bg-7-1543-2010.

[21] H. P. Freitag, M. J. McPhaden, P. E. PuIIen, "Fish-induced Bias In Acoustic Doppler Current Profiler Data," OCEANS 92 Proceedings-Mastering the Oceans Through Technology, 1992, pp. 712-717, doi: 10.1109/OCEANS.1992.607670.

[22] A. Y. Shcherbina, E. A. D'Asaro, S. Nylund, "Observing finescale oceanic velocity structure with an autonomous Nortek acoustic Doppler current profiler," Journal of Atmospheric and Oceanic Technology, Vol. 35, Issue 2, pp. 411-427, doi: 10.1175/JTECH-D-17-0108.1.

[23] L. Zedel, T. Knutsen, "Measurement of fish velocity using Doppler sonar," OCEANS 2000 MTS/IEEE Conference and Exhibition. Conference Proceedings, 2000, pp. 1951-1956 vol.3, doi: 10.1109/OCEANS.2000.882225.

[24] H. P. Freitag, P. E. Plimpton, M. J. McPhaden, "Evaluation of an ADCP fish-bias rejection algorithm," Proceedings of OCEANS '93, 1993, pp. II394-II397 vol.2, doi: 10.1109/OCEANS.1993.326127.

[25] T. E. Ryan, R. A. Downie, R. J. Kloser, G. Keith, "Reducing bias due to noise and attenuation in open-ocean echo integration data", 2015, ICES Jounral of Marine Science, Vol 72, Issue 8, pp. 2482–2493, doi: 10.1093/icesjms/fsv121.

[26] A. De Robertis, I. Higginbottom, "A post-processing technique to estimate the signal-to-noise ratio and remove echosounder background noise", ICES Journal of Marine Science, Vol. 64, Issue 6, 2007, pp. 1282–1291, doi: 10.1093/icesjms/fsm112.

[27] S. S. Urmy, J. K. Horne, D. H. Barbee, "Measuring the vertical distributional variability of pelagic fauna in Monterey Bay", ICES Journal of Marine Science, Vol. 69, Issue 2, 2012, pp. 184–196, doi: 10.1093/icesjms/fsr205.

[28] A. Roesch, H. Schmidbauer, "WaveletComp: Computational Wavelet Analysis", R package version 1.1, 2018, https://CRAN.R-project.org/package=WaveletComp.